Lead Alters Growth and Reduces Angiotensin II Receptor Density of Rat Aortic Smooth Muscle Cells (43938)

ROCCO V. CARSIA,*,[1] DANIEL FORMAN,* CARL E. HOCK,*,† ROBERT G. NAGELE,‡ AND PATRICK J. MCILROY§

Departments of Cell Biology, Medicine,† and Molecular Biology,‡ University of Medicine and Dentistry of New Jersey-School of Osteopathic Medicine, Stratford, New Jersey 08854, and Department of Biology,§ Camden College of Arts and Sciences-Rutgers University, Camden, New Jersey 08102*

Abstract. **Environmental lead (Pb^{2+}) contributes a small but significant risk to human hypertension. It is postulated that the hypertensinogenic action of Pb^{2+} may be due, in part, to its direct action on vascular smooth muscle cells. To investigate this hypothesis, freshly isolated rat aortic smooth muscle (RASM) cells were propagated in defined media containing one of two Centers for Disease Control–based concentrations of Pb^{2+} (as lead citrate): 100 and 500 μg Pb^{2+}/l (i.e., equivalent to 5.5 and 27.5 μg Pb^{2+}/dl blood; designated 100-RASM and 500-RASM). Control (CON-RASM) cells received sodium citrate. 500-RASM cells exhibited suppressed propagation and fell out of propagation synchrony with CON-RASM cells: when CON-RASM cell approached confluence (~90%), 500-RASM cell density was 6.4% that of CON-RASM cell density. By contrast, 100-RASM cells exhibited marked hyperplasia albeit this was not apparent until passage 3 (p3). Overall, when p3–p6 CON-RASM cells approached confluence, 100-RASM cell density was 107.6% greater than CON-RASM cell density. The protein content of CON-RASM and 100-RASM was not different, whereas that of 500-RASM cells was 29% greater than that of CON-RASM and 100-RASM cells. Phase-contrast microscopy revealed that 100 μg Pb^{2+}/l converted normal spindle-shaped/ribbon-shaped RASM cells into less spread, cobblestone-shaped, neointimal-like cells. Immunocytochemical analysis revealed that 100-RASM cells lacked or had markedly fewer actin cables, characteristic of rapidly dividing cells. In addition, Pb^{2+}-treated RASM cells exhibited altered membrane fatty acyl composition with a trend towards an increase (by as much as 50%) in membrane arachidonic acid. Interestingly, hyperplastic 100-RASM cells exhibited a 70.6% reduction in angiotensin II (Ang II) receptor concentration whereas the concentrations of α_1- and β-adrenergic and atrial natriuretic peptide (ANP) receptors were not affected. In addition, in experiments designed to control for Pb^{2+}-associated differences in RASM cell propagation, there was a concentration-dependent decrease in Ang II receptor concentration: for 100 and 500 μg Pb^{2+}/l, Ang II receptor concentration was decreased 39.6% and 65.5%, respectively. Thus, although Pb^{2+}, depending on its concentration, had contrasting effects on RASM cell propagation, it had a consistent, concentration-dependent inhibitory effect on Ang II receptor concentration. Recovery (r) from Pb^{2+} required at least two additional passages. At $p7_{1r}$, the enhanced propagation (+54%) and reduced Ang II receptor concentration (−49%) of 100r-RASM cells persisted. However, 500r-RASM cells exhibited a rebounded and enhanced (+37%) propagation with a concomitant reduction (−58%) in Ang II receptor concentration. These residual effects of Pb^{2+} were almost completely normalized with a second recovery passage (i.e., $p8_{2r}$). These effects of the Pb^{2+} appeared to be direct since conditioned medium from hyperplastic 100r- and 500r-RASM cells did not affect CON-RASM cell propagation or Ang II receptor parameters. Thus, depending on its concentration and duration in culture, Pb^{2+} can differentially alter vascular smooth muscle cell growth and can selectively reduce cellular Ang II receptor concentration.** [P.S.E.B.M. 1995, Vol 210]

[1] To whom requests for reprints should be addressed at Department of Cell Biology, UMDNJ-School of Osteopathic Medicine, 2 Medical Center Drive, Stratford, NJ 08084-1489.

Received October 24, 1994. [P.S.E.B.M. 1995, Vol 210]
Accepted July 10, 1995.

0037-9727/95/0000-0000$10.50/0

Lead (Pb^{2+}) continues to hold prominence as a major environmental and occupational health hazard. However, despite several decades of research, its multifaceted mechanisms of toxic action in several organ systems remain obscure.

The clinical literature is replete with associations between Pb^{2+} toxicity and hypertension. It is generally agreed that Pb^{2+} contributes a small but significant risk of cardiovascular disease to the population (1). However, its contribution may be amplified by other risk factors (2, 3). In addition, Pb^{2+} toxicity may be a confounding factor in understanding African-American–Caucasian differences in blood pressure studies (4).

It is postulated that the risk of cardiovascular disease contributed by Pb^{2+} is largely due to its induction of hypertension (1, 5–8). Concern, as adjudged by the Centers for Disease Control (CDC), occurs when blood Pb^{2+} concentrations approach and exceed 10 μg/dl (9). However, other epidemiological data suggest that concern needs to be focused at lower blood levels (7). In addition, the impact of the rate and duration of Pb^{2+} toxicity has been poorly studied. This is important in terms of the slow release of Pb^{2+} from bone (10) with advancing age and its possible role in postmenopausal hypertension. Furthermore, data indicate that even transient Pb^{2+} toxicity has a long-term effect in elevating blood pressure (11). Moreover, experimental evidence suggests that Pb^{2+} can accelerate the expression of hypertension in genetically susceptible individuals (12). However, despite its growing importance in the development of hypertension, the hypertensinogenic mechanisms of Pb^{2+} are poorly understood.

There are several plausible mechanisms concerning the hypertensinogenic actions of Pb^{2+}. (i) Although lead exerts toxic effects on several organ systems, those in the kidney are most insidious. Disruption of kidney function may lead to overall failure of electrolyte homeostasis and abnormalities in the renin-angiotensin system, thus contributing to hypertension (13). (ii) Pb^{2+} disrupts central nervous and peripheral nervous function (14), and produces an overall sympathetic nervous hyperactivity (15). Possibly, this contributes to neurogenic-induced hypertension. (iii) Pb^{2+} may have direct effects on vascular smooth muscle, thus increasing smooth muscle response to neural and/or hormonal stimuli and inducing neointimal properties.

The last postulated mechanism is supported by several pieces of evidence from *in vivo* and *in vitro* studies. For example, studies *in vivo* indicate that Pb^{2+} induces hypertension by increasing vascular tone (16–18) and vascular responsiveness to adrenergic agonists (15, 17, 18), and this is corroborated by *in vitro* studies (17, 18).

The intracellular changes underlying this increase in vascular tone are probably multiple but those concerned with calcium (Ca^{2+}) metabolism are prominent. For example, low concentrations of Pb^{2+} (~1 μ*M* [~10 μg/dl blood]), well within the range of concentrations considered a health problem (0–1 μ*M* [0–10 μg/dl blood]), greatly increase free Ca^{2+} in platelets (19). It can be postulated that Pb^{2+} has a similar effect on vascular smooth muscle cells. Pb^{2+} is known to interact with a number of intracellular proteins (20). Some of these targeted intracellular proteins are Ca^{2+}-binding proteins, notably calmodulin and Ca^{2+}-sensitive protein kinase C (20–22). Several Pb^{2+}-Ca^{2+} interactions with these proteins and the direct inhibitory effect of Pb^{2+} on Na^{+}-K^{+} ATPase (12, 23) result in an increase in intracellular Ca^{2+} in vascular smooth muscle (12, 18, 24).

In addition, there is evidence that Pb^{2+} acts as a divalent cation substitute in second messenger metabolism (20–22). For example, very low concentrations (pM) of Pb^{2+} can compete with zinc (Zn^{2+})-binding sites of protein kinase C (25) and thus activate protein kinase C (26). Evidence indicates that both an increase in intracellular Ca^{2+} (18, 27) and activation of protein kinase C (18, 28) enhance vascular smooth muscle growth and responsiveness. Furthermore, Pb^{2+} can compete with Ca^{2+} for calmodulin (20–22). The Pb^{2+}-calmodulin may activate or inhibit effector molecules. The role of calmodulin in advancing the cell cycle and regulating cell proliferation is well documented (29–32). Moreover, in a limited study of rabbit aortic smooth muscle cells, Pb^{2+} enhanced proliferation and increased cellular calmodulin content at the late G1 stage (33).

Thus, although there is considerable circumstantial clinical and experimental evidence supporting the notion that Pb^{2+} can alter vascular smooth muscle function, there have been no detailed investigations of this postulate. Accordingly, in the present study, we examined the influence of Pb^{2+} on early-passage rat aortic smooth muscle (RASM) cells. We report that Pb^{2+}, at a low CDC-based concentration (100 μg/l; i.e., 5.5 μg/dl blood), enhanced RASM cell propagation (+108%). This enhancement of RASM cell propagation persisted for one recovery passage (i.e., in the absence of Pb^{2+}). Concomitant with this enhancement of propagation was a consistent and selective suppression of cellular angiotensin II (Ang II) receptor concentration (−70.6%). In addition, Pb^{2+} induced alterations in the fatty acyl composition of RASM cell membranes, namely an increase in arachidonic acid and its precursor. Furthermore, Pb^{2+} induced alterations in RASM cell morphology and cytoskeletal architecture that are characteristic of rapidly dividing, neointimal-like vascular smooth muscle cells. Moreover, these actions of Pb^{2+} on RASM cells appear to

be direct since conditioned medium from recovery passage hyperplastic RASM cells did not alter control RASM cells. Interestingly, even a high concentration of Pb^{2+} (i.e., 500 μg/l [27.5 μg/dl blood]), which arrested RASM cell growth, was not toxic to RASM cells. Importantly, these effects of Pb^{2+} were normalized by two recovery passages.

Materials and Methods

Isolation of Rat Aortic Smooth Muscle Cells. Male Sprague-Dawley rats (~200–250 g) were housed in an isolation room maintained at a constant temperature and humidity and kept on a 12:12-hr light:dark cycle. Rats had free access to a commercially available diet and water.

Rats (10–15/experiment) were anesthetized with ketamine (90 mg/kg) and xylazine (10 mg/kg) and then euthanized by excising the heart and subsequent exsanguination. Their thoracic aortae were removed and trimmed free of adherent connective tissue and then processed for the isolation of RASM cells as described in detail elsewhere (34). In brief, the aortae were cut open longitudinally and the endothelial cell layer was removed using a cell scraper. The endothelium-free strips were incubated in a collagenase-elastase solution made up in penicillin/streptomycin-fortified Dulbecco's modified Eagle's medium (DMEM) (collagenase, type I [165 U/ml]; elastase, type III [15 U/ml]; soybean trypsin inhibitor [0.375 mg/ml]; BSA [2 mg/ml]; Sigma Chemical Co., St. Louis, MO) for 30 min at 37°C to free the adventitial layer. After removal of the adventitia, the tunica media was minced and placed in the collagenase-elastase solution. The minced tissue was digested for 3 hr with intermittent trituration (i.e., four times/hr) using a 10-ml pipet. At the end of the digestion period, the cells and residual tissue pieces were harvested (800 *g;* 10 min) and the resultant loose pellet was resuspended in complete medium (i.e., DMEM containing 10% fetal bovine serum [Hyclone Laboratories, Inc., Logan, UT], penicillin [100 U/ml], and streptomycin [100 μg/ml]) to a final concentration of 2–3 thoracic-aorta equivalents/ml. The resuspended tunica media cells and tissue fragments were plated into 100-mm plastic culture dishes (Falcon #3003) at 1 ml/dish. The material was spread over the surface of the dish by agitation and allowed to contact the surface for 1 hr at 37°C. After contact, cultures were carefully flooded with 5 ml of complete medium and then incubated for at least 2 days before feeding. RASM cells that migrated from the explant tissue fragments were left to propagate for up to 12 days, at which time they had achieved 70%–80% confluence. These cells were denoted as passage 0 (p0).

Propagation and Treatment of RASM Cells. For passage, cells were detached (0.25% trypsin in Dulbecco's Ca^{2+}-free phosphate buffered saline [PBS] [Sigma]), resuspended in complete medium and then plated at 5×10^4 cells/ml into T-75 tissue culture-treated polystyrene flasks (Falcon #3084). Addition to the basic complete medium were one of the following concentrations of Pb^{2+} (as lead citrate): 100 and 500 μg/l (i.e., ≈5.5 and 27.5 μg/dl blood). Control cells were passed in complete medium containing sodium citrate at a concentration having the same ionic strength as the 500 μg Pb^{2+}/l.

For most experiments, RASM cells (in complete medium with or without Pb^{2+}) were plated at 5×10^4 cells/ml into six-well multiwell surface-modified polystyrene culture plates (9.62 cm^2/well) (Falcon, Primaria; #3846) (1 ml/well). Cells were grown to near confluence (i.e., 80%–90% confluent). Cell morphology was routinely monitored and photographed using a Nikon Diaphot light microscope equipped with phase-contrast and Nomarski differential interference optics.

In some experiments designed to determine whether the growth-promoting effects of Pb^{2+} were mediated through the release of soluble growth factors, conditioned medium from hyperplastic recovery cells (i.e., in the absence of Pb^{2+}) was tested in CON-RASM cell culture. In brief, culture medium from subconfluent (80%–90%) hyperplastic 100- and 500-RASM cells after 2 days of culture was vacuum-filtered through a 0.22-μm cellulose acetate filter (Corning Inc., Corning, NY), mixed with fresh culture medium (1:1, v/v) and applied to subconfluent CON-RASM cells (5.2×10^3 cells/cm^2). Homologous conditioned medium from CON-RASM cells served as a control.

For estimates of propagation, RASM cells were harvested by mild trypsin treatment from randomly chosen wells (six wells/treatment group) at regular intervals and were counted with a hemacytometer. Trypan blue dye (0.4%) exclusion indicated that routinely greater than 98% of the cells were viable after trypsin-induced detachment. The resultant density of cells (number of cells/cm^2) served as an index of propagation. In all experiments, the last estimate or propagation for all treatment groups was determined when CON-RASM cells approached confluence (~90%), in order to avoid problems of contact inhibition.

Immunofluorescent Localization of Actin. RASM cells were plated at 5×10^4 cells/ml into two-well tissue culture chambers (2 ml/well) having a glass slide as a common floor (Nunc, Inc., Naperville, IL). Thus, every slide had both Pb^{2+}-treated and control cells. In most experiments, cells were allowed to attach to the glass and grow to about 80%–90% confluence. After reaching a desired density, cells were washed with Dulbecco's Ca^{2+}-free PBS and then fixed in ice-cold methanol for 3 min followed by ice-cold acetone for 2 min. Cells were air-dried and then rehydrated with Dulbecco's Ca^{2+}-free PBS. Next, cells were blocked with 1% BSA (in Ca^{2+}-free PBS) for 4

hr. After blocking, cells were incubated with α-smooth muscle actin antibody (monoclonal IgG2a, #A 2547, 1:50 titer in blocking solution; Sigma) at 4°C overnight. Then cells were washed for 1 hr with Ca^{2+}-free PBS and gentle agitation. After washing, cells were incubated with FITC-conjugated secondary antibody (#PF274 against IgG2a, 1:50 titer in blocking solution; The Binding Site Inc., San Diego, CA) in the dark at room temperature for 2 hr. Then, cells were washed with Ca^{2+}-free PBS and gentle agitation for 1 hr. After washing, slides were mounted and cells were examined under a fluorescent microscope (35).

Receptor Analysis. Ang II and β-adrenergic, α_1-adrenergic, and atrial natriuretic peptide (ANP) receptor number (i.e., cellular density, number of specific sites/cell) and affinity (K_a) were evaluated in intact RASM cells using methods published elsewhere (36). In brief, cultured cells were washed with Ca^{2+}-free PBS. Then warmed binding medium (DMEM containing 5 mg BSA/ml, 2 mg bacitracin/ml, and 1 m*M* hydroxyquinoline hemisulfate) was added to the cultures. Additions to the binding medium were the following radioligands and competing ligands (final incubation volume, 500 μl): (i) angiotensin II and ANP receptors—[^{125}I-Tyr^4, Ile^5]Ang II or [^{125}I-Tyr^{28}]rat ANP (50–100 p*M*) (DuPont NEN Research Products, Boston, MA) and various concentrations (0, 10^{-11}–10^{-5} *M*) of [Ile^5]Ang II or rat ANP, respectively (Peninsula Laboratories, Inc., Belmont, CA); (ii) β- and α_1-adrenergic receptors—various concentrations of [^{125}I]-(±)Iodocyanopinodol or [^{125}I]-HEAT, respectively (0–2500 p*M*) (DuPont NEN) with or without propranolol (200 μ*M*) or prazosin (119 μ*M*), respectively.

All binding reactions were carried out for 60–120 min with intermittent agitation at 37°C. Binding reactions were terminated by rapid washes with ice-cold Ca^{2+}-free PBS followed by solubilization of cells with 1 *N* NaOH-0.4% Triton X-100. Radioactivity was measured in a gamma counter.

Lipid Extraction and Analysis. RASM cell cultures (p6) were washed with Ca^{2+}-free PBS and then frozen (−80°C) until processing for lipid analysis. Lipids were extracted from frozen RASM cell cultures by the method of Bligh and Dyer (37). In brief, total phospholipids were separated from neutral lipids by thin-layer chromatography. Fatty acid methyl esters were prepared from phospholipids using 14% boron trifluoride in methanol. The fatty acid composition of the phospholipids was determined by gas chromatography using a Perkin-Elmer model 8500 gas chromatograph equipped with a 30 meter Omegawax 320 (Supelco, Inc., Bellefonte, PA) fused silica capillary column. The fatty acid composition of the samples was computed by integration and expressed as weight percent.

Cellular Protein Measurement. Subconfluent (~90%) RASM cells were harvested by mild trypsin treatment from randomly chosen wells (six wells/treatment group) at regular intervals and were counted with a hemacytometer. They were then washed twice with Ca^{2+}-free PBS and pelleted (800 *g*, 15 min, 4°C). Cell pellets were processed for the measurement RASM cell protein content (38) using commercially available reagent (Bio-Rad Laboratories, Hercules, CA).

Data Analysis. All receptor binding data were statistically analyzed using the LIGAND computer program (39). All other data were statistically analyzed by analysis of variance using standard computer-based programs. Means were separated by the Newman-Keuls test and were deemed significantly different at $P < 0.05$.

Results

Studies addressed the hypothesis that Pb^{2+} directly enhances vascular smooth muscle growth and function. Accordingly, we measured the influence of two CDC-based concentrations of Pb^{2+}, 100 and 500 μg/l (as lead citrate) (i.e., ≈5.5 and 27.5 μg/dl blood) on RASM cell propagation and basic parameters (affinity, as determined by the association constant, K_a; cellular concentration, i.e., sites/cell) of RASM cell Ang II and β-adrenergic, α_1-adrenergic, and ANP receptors. Treated cells were designated as 100-RASM and 500-RASM, respectively. Control RASM (CON-RASM) cells received sodium citrate at a concentration equivalent to the higher lead citrate concentration.

Table I shows the effect of Pb^{2+} on RASM cells propagated on surface-modified polystyrene (Falcon Primaria, #3846). Overall, the density of 100-RASM cells was 107.6% ± 31.9% (mean ± SEM) greater than that of nearly confluent (~90%) CON-RASM cells. Note that the enhanced propagation was not apparent until p3. By contrast, 500-RASM cells fell out of propagation synchrony. Thus, over the six passages, 500-RASM cells were passed only twice and never reached confluence. For example, at 18 days after plating, 500-RASM cell density was only 24.8% of the average control RASM cell density (~90% confluent), and when harvested at ~90% RASM cell confluence, was only 6.4% of control RASM cell density.

Morphologically, 100-RASM cells have features closely resembling those of neointimal RASM cells reported by others (34, 40). Figure 1 shows phase-contrast photomicrographs of p5 CON-RASM cells, 100-RASM cells, and 500-RASM cells. Compared with CON-RASM cells (Fig. 1A), which exhibited well-spread, sharply polygonal, spindle-shaped/ribbon-shaped profiles, a characteristic of normal rat tunica media cells in culture (34, 40), 100-RASM cells showed less spreading, smaller and more rounded, cobblestone-shaped profiles, a characteristic of neointimal

Table I. Influence of Pb^{2+} on RASM Cell Propagation

Passage	Hours[a]	Concentration of Pb^{2+} (μg/l)		
		Control (0)	100	Δ %[b]
2	218	67,250 ± 4,180	61,290 ± 4,830	−8.9
3	170	36,710 ± 1,910	60,090 ± 3,790[c]	+63.7
4	194	43,740 ± 1,940	130,200 ± 7,250[c]	+197.7
5	156	60,290 ± 2,450	96,760 ± 3,550[c]	+60.5
6	174	38,380 ± 1,640	80,170 ± 3,910[c]	+108.9

Note. RASM cells were plated at 5×10^4 cells/ml (1 ml) into six-well multiwell, surface modified polystyrene plates (Falcon Primaria; #3846). Data (number of cells/cm^2) are the means ± SEM of six randomly chosen wells from a representative of three independent propagation studies.

[a] Hours indicate the time elapsed since passage plating at which control RASM cells appeared 80%–90% confluent.

[b] Δ%, indicates percent change versus control.

[c] Significantly different ($P < 0.05$) from corresponding control value.

cells. In addition, 100-RASM cells exhibit numerous mitotic figures despite their high density (Fig. 1B). Indeed, 100-RASM cells tend to form hillocks and exhibited decreased contact inhibition at clearly overconfluent densities compared to CON-RASM cells at nearly confluent densities (images not shown). By contrast, 500-RASM cells exhibit wide variations in the degree of spreading with ruffled borders. Profiles range from grotesque to unremarkable (Fig. 1C).

To determine whether 100-RASM cells were actually smaller than CON-RASM cells, the protein content of isolated cells was measured. The protein content of CON-RASM and 100-RASM was not different whereas that of 500-RASM cells was 29% greater ($P < 0.05$) than that of CON-RASM and 100-RASM cells (protein content [$\mu g/10^6$ cells] was respectively 151.5 ± 5.9, 160.8 ± 6.4 and 200.5 ± 5.1 [means ± SEM from 18 randomly chosen wells, six wells from each of three experiments]).

Figure 2 shows immunofluorescent localization of α-smooth muscle actin in p5 control RASM cells (Fig. 2, A and D), 100-RASM cells (Fig. 2, B and E), and 500-RASM cells (Fig. 2, C and F). Compared with control cells, 100-RASM cells exhibited fewer, finer, and less prominent actin-containing cytoplasmic fibers (actin cables), a characteristic of rapidly dividing cells. Collectively, Fig. 1 and 2 suggest that low concentrations of Pb^{2+} induced neointimal-like properties in vascular smooth muscle cells. By contrast, 500-RASM cells possessed actin cables that were thick but less prominent and disorganized compared with control RASM cells. Another prominent feature of 500-RASM cells was the greater incidence of cells having two or divided nuclei (Fig. 2C; Table II), suggesting that complete mitosis was arrested by the high concentration of Pb^{2+}. This might also explain the greater protein content of 500-RASM cells compared to CON- and 100-RASM cells (*vide supra*).

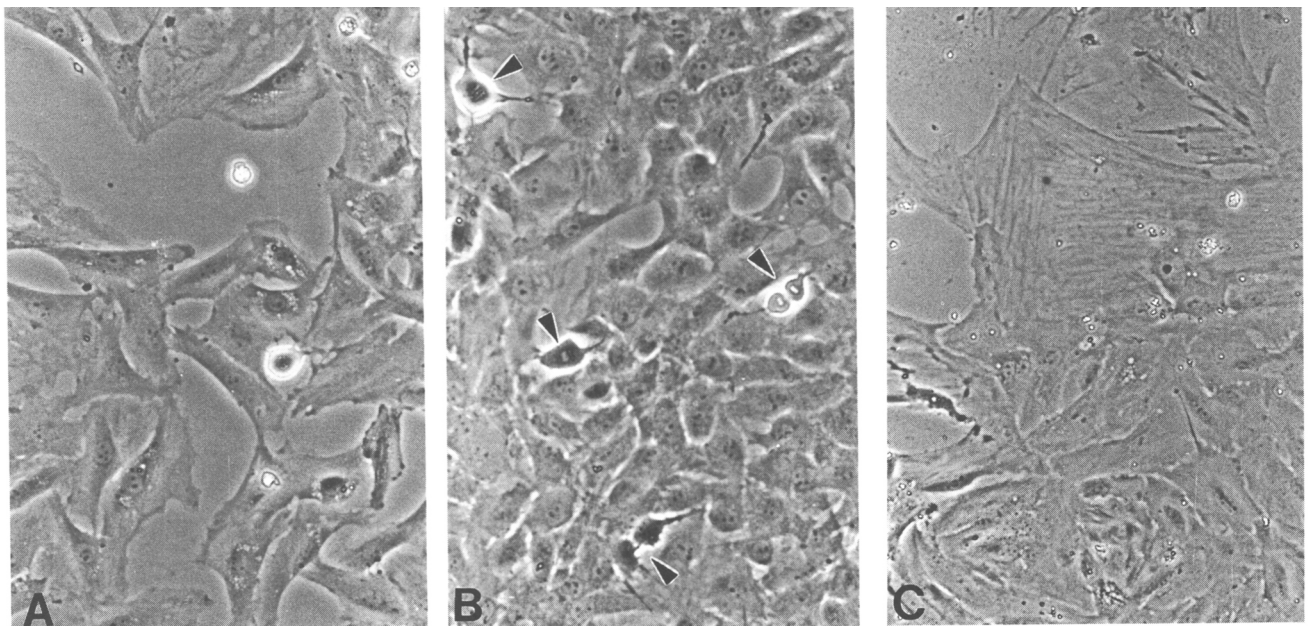

Figure 1. Phase-contrast photomicrographs of P5 control RASM cells (A), 100-RASM cells (B), and 500-RASM cells (C). Note the numerous mitotic figures (arrow heads) of 100-RASM cells. Original objective magnification: ×10 for all.

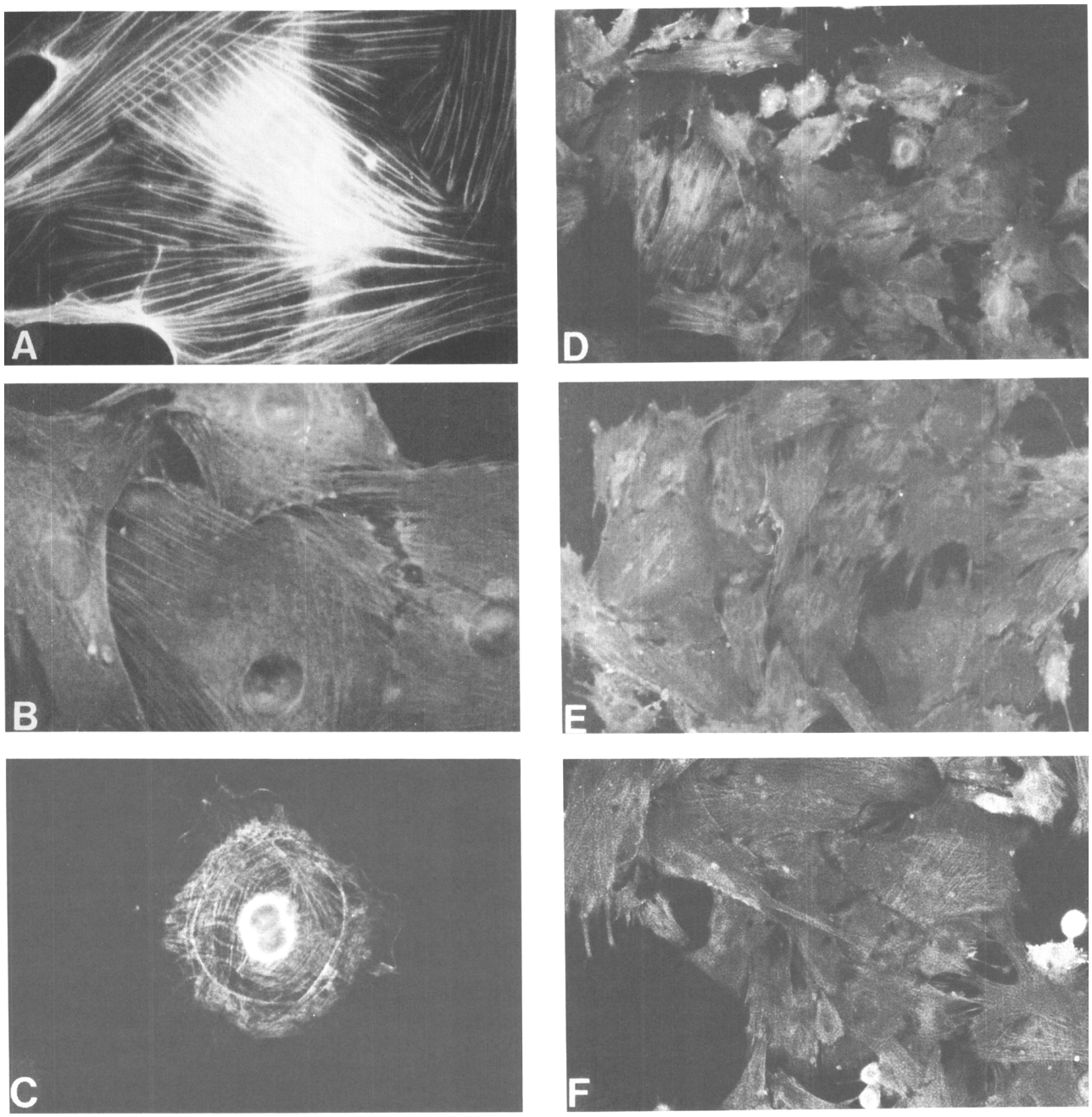

Figure 2. Immunofluorescent localization of α-smooth muscle actin in P5 control RASM cells (A and D), 100-RASM cells (B and E), and 500-RASM cells (C and F). Original objective magnification: ×40 for A, B, and C, and ×10 for D, E, and F.

In order to assess the influence of Pb^{2+} on some aspect of RASM cell function, we evaluated Ang II and β-adrenergic receptors in various passages of control and Pb^{2+}-treated RASM cells. The data are shown in Table III. Pb^{2+} (100 μg/l) did not alter the affinities of these receptors. However, Pb^{2+} decreased the cellular concentration of Ang II receptors without affecting the cellular density of β-adrenergic receptors. A significant Pb^{2+}-induced decrease in cellular Ang II receptor density occurred at p3 and persisted through p6. Interestingly, this Pb^{2+}-induced decrease in cellular Ang II receptor concentration was coincident with the Pb^{2+}-induced increase in RASM cell propagation (Table I) (i.e., both occurring at p3).

It is possible that the effect of Pb^{2+} on cellular Ang II receptor concentration was mediated by its enhancement of RASM cell propagation, clustering and crowding. To investigate this postulate, propagation experiments were conducted in which the plating density was adjusted for each passage to compensate for the stimulatory or inhibitory effect of Pb^{2+}, depending on its concentration. Thus, CON-RASM cells were plated at $\sim 1 \times 10^5$ cells/ml, 100-RASM cells were plated at $\sim 5 \times 10^4$ cells/ml, and 500-RASM cells were

Table II. Influence of Pb^{2+} on the Incidence of RASM Cells (%) Containing Two or Divided Nuclei

Field[a]	Pb^{2+} concentration (μg/l)		
	Control (0)	100	500
>10 cells/cluster	1.7 ± 0.6 (n = 20)	3.5 ± 0.8 (n = 25)	24.8 ± 4.7 (n = 20)[b]
1 to ≤10 cells/cluster	17.3 ± 6.7 (n = 35)	22.1 ± 6.7 (n = 35)	51.3 ± 10.5 (n = 25)[b]

Note. RASM cells were propagated for the first five to six passages (p1–p6) in the presence of the indicated concentrations of Pb^{2+}. Cells were then plated at 5 × 10^4 cells/ml into two-well tissue culture chambers (2 ml/well) having a glass slide as a common floor such that each slide had both Pb^{2+}-treated and control cells. In most experiments, cells were allowed to attach to the glass and grow to about 80%–90% confluence. Cells were then processed for immunofluorescent localization of α-smooth muscle actin as described in Materials and Methods.

[a] Random fields from three propagation studies ending with either p5 or p6 cells containing either single cells or clusters of cells were photographed and then analyzed for the occurrence of RASM cells bearing two or divided nuclei (see Fig. 2C) (number of cells bearing two or divided nuclei/total number of cells per field expressed as percent; n = number of fields analyzed).

[b] Significantly different ($P < 0.05$) from corresponding control value.

plated at ~5 × 10^5 cells/ml. Thus, for p5 and p6, roughly equivalent over-confluent cell densities were achieved for each treatment group. Ang II receptors were evaluated and the results are shown in Table IV. Overall, there was a concentration-dependent inhibitory effect of Pb^{2+} on cellular Ang II receptor concentration: for 100 and 500 μg Pb^{2+}/l, cellular Ang II receptor concentration was reduced by 39.6% and 65.5%, respectively ($P < 0.05$).

In other experiments, the effect of Pb^{2+} on α_1-adrenergic and ANP receptors, as well as on Ang II and β-adrenergic receptors, was investigated. Consistent with the data presented here, Pb^{2+} decreased the cellular concentration of Ang II receptors but did not affect β-adrenergic receptors (Table V). In addition, it had no effect on the affinity and cellular density of α_1-adrenergic receptors. However, 500 μg Pb^{2+}/l had an inhibitory effect on the cellular density of ANP receptors (Table V) but did not affect ANP receptor affinity (data not shown).

Interestingly, even a high concentration of Pb^{2+} (i.e., 500 μg/l [27.5 μg/dl blood]), which arrested RASM cell growth, was not toxic to RASM cells. Importantly, these effects of Pb^{2+} were normalized by two recovery passages. However, noteworthy is the fact that recovery 100-RASM cells exhibited a persistent enhanced propagation and suppressed 500-RASM cells exhibited a rebound enhanced propagation (Table VI). Thus, prior treatment with 100 and 500 μg Pb^{2+}/l enhanced recovery RASM cell propagation by 48.0% and 34.7%, respectively, for one passage ($p7_{1r}$). This enhancement in propagation was accompanied by a decrease in cellular concentration of Ang II receptors (control: [2.02 ± 0.32] × 10^4 sites/cell; 100 μg Pb^{2+}/l: [1.03 ± 0.16] × 10^4 sites/cell [−48.9%]; 500 μg Pb^{2+}/l: [0.89 ± 0.12] × 10^4 sites/cell [−56.0%] [mean ± SEM; $P < 0.05$]). However, at the second recovery passage ($p8_{2r}$), these residual effects of Pb^{2+} on Ang II receptors were completely normalized (control: [2.14 ± 0.36] × 10^4 sites/cell; 100 μg Pb^{2+}/l: [2.63 ± 0.30] × 10^4 sites/cell; 500 μg Pb^{2+}/l: [2.55 ± 0.73] × 10^4 sites/cell [mean ± SEM]). This normalization of cellular concentration of Ang II receptors was coincident with the normalization of RASM cell propagation.

These actions of Pb^{2+} on RASM cells appeared to be direct and not mediated by stabile soluble growth factors. Compared with homologous conditioned medium from CON-RASM cells, pooled conditioned medium from recovery passage hyperplastic 100- and 500-RASM cells did not alter final CON-RASM cells density ([11.22 ± 1.20] × 10^4 cells/cm^2 *vs* [11.71 ± 1.18] × 10^4 cells/cm^2, respectively) or Ang II receptor parameters (K_a: [2.45 ± 0.42] × 10^9 M^{-1} *vs* [2.48 ± 0.36] ×

Table III. Influence of Pb^{2+} on Affinity (K_a) and Concentration of RASM Cell Ang II and β-Adrenergic Receptors

Passage	Ang II receptors				β-Adrenergic receptors			
	K_a (10^9 M^{-1})		Concentration (10^4 sites/cell)		K_a (10^9 M^{-1})		Concentration (10^5 sites/cell)	
	Control	100 μg Pb^{2+}/l	Control	100 μg Pb^{2+}/l	Control	100 μg Pb^{2+}/l	Control	100 μg Pb^{2+}/l
2	2.71 ± 0.29	2.49 ± 0.31	6.87 ± 0.12	6.58 ± 0.15	2.68 ± 0.13	2.98 ± 0.41	5.51 ± 1.10	9.48 ± 2.95
3	1.62 ± 0.71	1.56 ± 0.18	6.11 ± 0.42	5.08 ± 0.38[a]	2.63 ± 0.34	2.04 ± 0.53	6.13 ± 3.11	10.50 ± 1.37
4	3.12 ± 0.34	3.10 ± 0.51	3.71 ± 0.22	0.82 ± 0.08[a]	3.13 ± 0.46	2.74 ± 0.52	4.81 ± 1.83	4.14 ± 1.62
5	2.55 ± 0.46	3.08 ± 0.52	3.68 ± 0.37	1.00 ± 0.10[a]	2.14 ± 0.39	2.64 ± 0.51	9.22 ± 3.10	4.69 ± 1.98
6	2.24 ± 0.28	2.19 ± 0.26	6.24 ± 0.47	2.23 ± 0.16[a]	2.49 ± 0.41	2.74 ± 0.58	7.18 ± 4.33	6.61 ± 3.98

Note. Binding studies were performed directly on cultured RASM cells at approximately 180 hr after passage plating (80%–90% confluent) as described in Materials and Methods. Data are the means ± SEM derived from three propagation studies. Binding isotherms were statistically analyzed by the LIGAND computer program (39).

[a] Significantly different ($P < 0.05$) from corresponding control value.

Table IV. Influence of Pb^{2+} on the Concentration of Ang II Receptors of Equivalent Densities of RASM Cells

Pb^{2+} concentration (μg/l)	RASM cell density (cells/cm²)	Concentration of cellular Ang II receptors (10^4 sites/cell)
Control (0)	131,200 ± 8,630	3.13 ± 0.24
100	132,000 ± 8,440	1.89 ± 0.21[a]
500	137,300 ± 9,150	1.08 ± 0.09[a]

Note. RASM cells were propagated with the indicated concentrations of Pb^{2+} for four passages. In each passage, cells were plated at 1×10^5, 5×10^4, and 5×10^5 cells/well (1 ml) for 0 (control), 100, and 500 μg Pb^{2+}/l, respectively, in order to normalize differences in propagation rates. Ang II binding studies were performed directly on cultured RASM cells at passages 5 and 6 in which roughly equivalent over-confluent RASM cell densities were achieved for each Pb^{2+} concentration. Data (pooled from passages 5 and 6) are the means ± SEM from three propagation studies. Ang II–binding isotherms were statistically analyzed by the LIGAND computer program (39).
[a] Significantly different ($P < 0.05$) from corresponding control value.

10^9 M^{-1}, respectively; concentration [10^4 sites/cell]: 4.33 ± 0.37 *vs* 3.94 ± 0.39, respectively) (means ± SEM of parameter estimates from three experiments).

Since soluble stabile growth factors did not appear to mediate the enhancement of RASM cell propagation induced by Pb^{2+}, we investigated the postulate that lipid mediators were involved. For example, enhanced entry of arachidonic acid into the 12-lipoxygenase pathway may be an important mechanism for augmentation of vascular smooth muscle growth induced by diverse factors such as high plasma glucose and Ang II (41). As a first step in the investigation of this postulate, we analyzed the fatty acyl composition of RASM cells. Interestingly, Pb^{2+} induced significant alterations in the unsaturated fatty acyl composition of RASM cells (Table VII). For example, 18:1 (ω-9) was decreased 21.7% ($P < 0.05$). By contrast, 18:2 (ω-6) linoleic acid), a precursor for arachidonic acid (20:4 [ω-6]), was increased 21.1% ($P < 0.05$). Indeed, this increase was consistent with the trend of an increase (~50%; $P = 0.08$) in arachidonic acid. The data suggest that the actions of Pb^{2+} in RASM cells may be mediated, in part, by alterations in the metabolism of lipid mediators.

Discussion

Pb^{2+}, depending on its concentration, had divergent effects on RASM cell propagation: 100 μg Pb^{2+}/l enhanced RASM cell propagation whereas 500 μg Pb^{2+}/l depressed propagation, presumably in part due to an arrest in cytokinesis. This observation is not surprising considering the multiple cellular loci of Pb^{2+} action and the Pb^{2+} concentration–dependent sensitivity of these loci (20–22). Conceivably, Pb^{2+} has direct aberrant growth factor properties that circumvent and subvert the normal cascade and balance of second-messenger, second-messenger-effector, and tensegrity (cytoskeletal signaling)-dependent events.

Prior treatment with 100 μg Pb^{2+}/l and 500 μg Pb^{2+}/l caused a persistent enhancement and rebound enhancement, respectively, of RASM cell propagation for one recovery passage. It is not clear whether this was due to mnemonic alterations in cellular function induced by Pb^{2+} or to the gradual dilution of Pb^{2+} influence on cellular function.

Although Pb^{2+}, depending on its concentration, had divergent influences on propagation, it had a consistent and fairly selective inhibitory effect on RASM cellular Ang II receptor density, regardless of concentration. This apparent selective inhibitory effect of Pb^{2+} on cellular Ang II receptor density is noteworthy. Although Ang II has been postulated to be an important growth factor of vascular smooth muscle cells (42–45), its precise role had evaded investigators. Recent evidence suggests that enhanced endogenous growth factor expression may mediate the growth-inducing effects of Ang II on vascular smooth muscle cells (43, 44, 46). In this connection, other recent work indicates that growth factors, that are known enhancers of RASM cell proliferation, markedly downregulate gene expression and destabilize mRNA for the

Table V. Influence of Pb^{2+} on the Concentration (10^4 sites/cell) of Ang II, β-Adrenergic, α_1-Adrenergic, and ANP Receptors of RASM Cells

Receptor	Pb^{2+} concentration (μg/l)		
	Control (0)	100	500
Ang II	5.32 ± 0.32	2.28 ± 0.18[a]	1.62 ± 0.13[a]
β-Adrenergic	158.96 ± 31.13	149.72 ± 27.81	160.57 ± 37.15
α_1-Adrenergic	7.03 ± 1.59	7.65 ± 0.97	7.71 ± 1.25
ANP	3.43 ± 0.93	2.45 ± 0.49	1.70 ± 0.26[a]

Note. RASM cells were propagated with the indicated concentrations of Pb^{2+} for four passages. In each passage, cells were plated at 1×10^5, 5×10^4, and 5×10^5 cells/well (1 ml) for 0 (control), 100, and 500 μg Pb^{2+}/l, respectively, in order to normalize differences in propagation rates. Binding studies were performed directly on cultured RASM cells at Passages 5 and 6. Data (pooled from Passages 5 and 6) are the means ± SEM from three propagation studies. Binding isotherms were statistically analyzed by the LIGAND computer program (39).
[a] Significantly different ($P < 0.05$) from corresponding control value.

Table VI. Recovery of RASM Cell Propagation from Pb^{2+}

Passage	Hours[a]	Pb^{2+} concentration in p1 through p6 (μg/l)				
		Control (0)	100	Δ%[b]	500	Δ%[b]
7_{1r}	92	1.02 ± 0.07	1.43 ± 0.09[c]	+40.2	1.35 ± 0.08[c]	+32.4
	140	3.82 ± 0.15	5.58 ± 0.18[c]	+46.1	5.23 ± 0.26[c]	+36.9
	193	9.58 ± 0.24	16.16 ± 1.00[c]	+68.7	13.25 ± 0.54[c]	+38.3
	217	23.43 ± 0.85	32.14 ± 1.14[c]	+37.2	30.67 ± 1.26[c]	+30.9
8_{2r}	172	23.86 ± 0.93	25.29 ± 1.61	+6.0	19.27 ± 0.90[c]	−19.2
	192	34.39 ± 1.04	37.16 ± 1.41	+8.1	36.86 ± 1.08	+7.2
	242	35.67 ± 1.75	34.76 ± 1.81	−2.6	34.50 ± 1.63	−3.3

Note. RASM cells were propagated for the first six passages (p1–p6) in the presence of the indicated concentrations of Pb^{2+}. Cells were then propagated in the absence of Pb^{2+} for an additional two recovery (r) passages designated $p7_{1r}$ and $p8_{2r}$. At each recovery passage, cells were plated at 2.5×10^4 cells/ml (1 ml) into six-well multiwell, surface modified polystyrene plates (Falcon Primaria; #3846). Data (10^4 cells/cm^2) are the means ± SEM of six randomly chosen wells from a representative of three independent propagation studies.

[a] Hours indicate the time elapsed since passage plating at which control RASM cells appeared 80%–90% confluent.

[b] Δ%, percentage change versus control.

[c] Significantly different ($P < 0.05$) from corresponding control value.

vascular type-1 Ang II receptor (47), which may be an important negative feedback mechanism in Ang II–induced vascular smooth muscle growth. In the present study, the mechanism of Pb^{2+}-induced reduction in RASM cell Ang II receptor concentration is unknown, albeit it does not appear to be mediated by growth factors. However, Pb^{2+}, like some growth factors, may operate through common intracellular signaling mechanisms leading to reduced Ang II receptor expression. In addition, although the previously mentioned mechanism may operate here (47), other plausible mechanisms deserve attention. For instance, in the type-1 Ang II receptor, the carboxyterminus, a region implicated in desensitization and downregulation (48), has potential phosphorylation sites for protein kinase C (48) and is a substrate for the Src family of tyrosine kinases (49). Conceivably, Pb^{2+} competes with Zn^{2+}-binding sites of protein kinase C (25), thus activating the enyzme (26). In addition, in some tissues, Src is regulated by a Zn^{2+}-dependent tyrosine kinase (50), another potential site of Pb^{2+} action. Conceivably, both protein kinase C and Src pathways converge to downregulate the vascular type-1 Ang II receptor and both pathways are enhanced by Pb^{2+}.

Further emphasizing the selective action of Pb^{2+} on RASM cell Ang II receptors is the fact that α_1-adrenergic receptors, which like type-1 Ang II receptors, are coupled to mobilization of intracellular Ca^{2+} (51, 52), have potential phosphorylation sites for protein kinase C (53, 54) and are implicated in vascular smooth muscle cell growth (55), are not affected by Pb^{2+} (Table V). Since Pb^{2+}, depending on its concentration, can dissociate RASM cell propagation from cellular Ang II receptor density, it may serve as a new "tool" for elucidating the relationship between vascular smooth muscle proliferation and the mechanisms regulating Ang II receptor expression.

Interestingly, there was a trend for Pb^{2+} to increase arachidonic acid in RASM cell membranes. This is noteworthy since recent work suggests that enhanced entry of arachidonic acid into the 12-lipoxygenase pathway may be an important mecha-

Table VII. Influence of Pb^{2+} on the Fatty Acyl Composition of Membrane Phospholipids Derived from RASM Cells

Fatty acid	Pb^{2+} concentration (μg/l)		
	Control (0)	100	500
13:0	23.03 ± 8.52	13.00 ± 2.09	28.55 ± 3.05
14:0	2.92 ± 1.53	2.52 ± 0.52	1.15 ± 0.20
14:1	0.29 ± 0.17	1.19 ± 0.48	0.95 ± 0.13
16:0	9.30 ± 1.42	11.07 ± 1.12	10.94 ± 0.36
16:1 (ω-7)	4.86 ± 0.67	4.44 ± 0.63	5.59 ± 0.28
18:0	12.13 ± 2.77	9.49 ± 0.69	9.26 ± 0.35
18:1 (ω-9)	22.52 ± 1.70	20.40 ± 2.10	17.64 ± 0.43[a]
18:1 (ω-11)	4.47 ± 2.68	8.35 ± 1.20	9.71 ± 0.55
18:2 (ω-6)	0.57 ± 0.25	0.49 ± 0.03	1.26 ± 0.07[a]
20:1	0.61 ± 0.35	0.95 ± 0.13	0.86 ± 0.16
20:3 (ω-3)	0.35 ± 0.23	0.46 ± 0.08	0.32 ± 0.19
20:4 (ω-6)	2.05 ± 0.19	2.43 ± 0.68	3.11 ± 0.53[b]
20:5 (ω-3)	0.79 ± 0.72	0.60 ± 0.54	0.22 ± 0.20
22:6 (ω-3)	0.57 ± 0.35	0.88 ± 0.44	0.30 ± 0.25

Note. RASM cells were propagated with the indicated concentrations of Pb^{2+} for five passages. In each passage, cells were plated at 1×10^5, 5×10^4, and 5×10^5 cells/well (1 ml) for 0 (control), 100, and 500 μg Pb^{2+}/l, respectively, in order to normalize differences in propagation rates. At p6, cells were washed, snap frozen, and then harvested and processed for the determination of fatty acyl composition as described in Materials and Methods. Values are the weight percentage of total fatty acids in cellular phospholipids and are the means ± SEM of four propagation cultures. Fatty acids are designated by chain length: number of double bonds with the number in parentheses representing the number of carbon atoms between the terminal double bond and the methyl group. The unsaturation index (Σ [weight percentage of unsaturated fatty acid × number of double bonds]) was not different between groups: 51 ± 9 (control), 56 ± 9 (100 μg Pb^{2+}/l) and 53 ± 5 (500 μg Pb^{2+}/l).

[a] Significantly different ($P < 0.05$) from corresponding control value.

[b] $P = 0.08$ *vs* corresponding control value.

nism for enhanced vascular smooth muscle cell growth induced by Ang II and for accelerated vascular disease produced by Ang II in certain disease states (41).

The disparate effects of the two concentrations of Pb^{2+} on actin organization deserves some attention. Possibly, cytoskeletal organization is better correlated with propagation than is cellular Ang II receptor density. For example, there is an emerging role of cytoskeletal-associated proteins in the growth response of vascular smooth muscle cells to Ang II (56). In addition, cyclic mechanical strain is an efficacious stimulator of vascular smooth muscle cell proliferation (57). Thus, it is equally plausible that Pb^{2+} acts at intracellular loci at which tensegrity (cytoskeletal signaling) and vasoregulatory molecule/growth factor signaling converge. This and other complex hypotheses raised here on the mechanisms of action of Pb^{2+} on vascular smooth muscle cells await further investigation.

This work was supported by USDA Grant 91-37206-6800.

We thank Dr. John S. Ellis and his vivarium staff for excellent animal care. In addition, we thank Ms. Andrea Hulse for photomicrography.

1. Schwartz J. Lead, blood pressure, and cardiovascular disease in men and women. Environ Health Perspect **91**:71–75, 1991.
2. Apostoli P, Maranelli G, Dei Cas L, Micciolo R. Blood lead and blood pressure: A cross sectional study in a general population group. Cardiologia **35**:597–603, 1990.
3. Maheswaran R, Gill JS, Beevers DG. Blood pressure and industrial lead exposure. Am J Epidemiol **137**:645–653, 1993.
4. Sorel JE, Heiss G, Tyroler HA, Davis WB, Wing SB, Ragland DR. Black-white differences in blood pressure among participants in NHANES II: The contribution of blood lead. Epidemiology **2**:348–352, 1991.
5. Beattie AD, Campbell BC, Goldberg A, Moore MR. Blood-lead and hypertension. Lancet **2**:1–3, 1976.
6. Neri LC, Hewitt D, Orser B. Blood lead and blood pressure: Analysis of cross-sectional and longitudinal data from Canada. Environ Health Perspect **78**:123–126, 1988.
7. Sharp DS, Osterloh J, Becker CE, Bernard B, Smith AH, Fisher JM, Syme SL, Holman BL, Johnston T. Blood pressure and blood lead concentration in bus drivers. Environ Health Perspect **78**:131–137, 1988.
8. Kopp SJ, Barron JT, Tow JP. Cardiovascular actions of lead and relationship to hypertension: A review. Environ Health Perspect **78**:91–99, 1988.
9. Centers for Disease Control. Preventing Lead Poisoning in Young Children. Atlanta, GA: U.S. DHHS, Public Health Service, Centers for Disease Control, 1991.
10. Wedeen RP. Bone lead, hypertension, and lead nephropathy. Environ Health Perspect **78**:57–60, 1988.
11. Hu H. A 50-year follow-up of childhood plumbism. Hypertension, renal function, and hemoglobin levels among survivors. Am J Dis Child **145**:681–687, 1991.
12. Nakhoul F, Kayne LH, Brautbar N, Hu MS, McDonough A, Eggena P, Golub MS, Bergeer M, Chang CT, Jamgotchian N. Rapid hypertensinogenic effect of lead: Studies in the spontaneously hypertensive rat. Toxicol Industrial Health **8**:89–102, 1992.
13. Nolan CV, Shaikh ZA. Lead nephrotoxicity and associated disorders: Biochemical mechanisms. Toxicology **73**:127–146, 1992.
14. Lilbergeld EK. Mechanisms of lead neurotoxicity, or looking beyond the lamppost. FASEB J **6**:3201–3206, 1992.
15. Boscolo P, Carmignani M. Neurohumoral blood pressure regulation in lead exposure. Environ Health Perspect **78**:101–106, 1988.
16. Victery W, Vander AJ, Shulak JM, Schoeps P, Julius S. Lead, hypertension, and the renin-angiotensin system in rats. J Lab Clin Med **99**:354–362, 1982.
17. Webb RC, Winquist RJ, Victery W, Vander AJ. *In vivo* and *in vitro* effects of lead on vascular reactivity in rats. Am J Physiol **241**:H211–H216, 1981.
18. Chai SS, Webb RC. Effects of lead on vascular reactivity. Environ Health Perspect **78**:85–89, 1988.
19. Dowd TL, Gupta RK. 19F-NMR study of the effect of lead on intracellular free calcium in human platelets. Biochim Biophys Acta **1092**:341–346, 1991.
20. Goering P. Lead-protein interactions as a basis for lead toxicity. Neurotoxicol **14**:45–60, 1993.
21. Simons TJB. Lead-calcium interactions in cellular lead toxicity. Neurotoxicology **14**:77–86, 1993.
22. Goldstein GW. Evidence that lead acts as a calcium substitute in second messenger metabolism. Neurotoxicol **14**:97–102, 1993.
23. Caspers ML, Kwaiser TM, Grammas P. Control of [^{3}H]ouabain binding to cerebromicrovascular (Na^+-K^+)-ATPase by metal ions and proteins. Biochem Pharmacol **39**:1891–1895, 1990.
24. Tomera JF, Harakal C. Mercury- and lead-induced contraction of aortic smooth muscle *in vitro*. Arch Int Pharmacodyn Therap **283**:295–302, 1986.
25. Hubbard SR, Bishop WR, Kirschmeier P, George SJ, Cramer SP, Hendrickson WA. Identification and characterization of zinc binding sites in protein kinase C. Science **254**:1776–1779, 1991.
26. Markovac J, Goldstein GW. Picomolar concentrations of lead stimulate brain protein kinase C. Nature **334**:71–73, 1988.
27. Heagerty AM. Angiotensin II: Vasoconstrictor or growth factor? J Cardiovasc Pharmacol **18**(Suppl 2):S14–S19, 1991.
28. Andrea JE, Walsh MP. Protein kinase C of smooth muscle. Hypertension **20**:585–595, 1992.
29. Chafouleas JG, Bolton WE, Hidaka H, Boyd AE, Means AR. Calmodulin and the cell cycle: Involvement in regulation of cell cycle progression. Cell **28**:41–50, 1982.
30. Sasaki Y, Hidaka H. Calmodulin and cell proliferation. Biochem Biophys Res Commun **104**:451–456, 1982.
31. Chafouleas JG, Lagace L, Bolton WE, Boyd AE, Means AR. Changes in calmodulin and it mRNA accompany reentry of quiescent (G0) cells into the cell cycle. Cell **36**:73–81, 1984.
32. Rasmussen CD, Means AR. Calmodulin is involved in regulation of cell proliferation. EMBO J **6**:3961–3968, 1987.
33. Lu KP, Zhao SH, Wang DS. The stimulatory effect of heavy metal cations on proliferation of aortic smooth muscle cells. Sci China (Series B, Chem Life Sci Earth Sci) **33**:303–310, 1990.
34. Schwartz SM, Foy L, Bowen-Pope DF, Ross R. Derivation and properties of platelet-derived growth factor-independent rat smooth muscle cells. Am J Pathol **136**:1417–1428, 1990.
35. Owens GK, Loeb A, Gordon D, Thompson MN. Expression of smooth muscle-specific α-isoactin in cultured vascular smooth muscle cells: Relationship between growth and cytodifferentiation. J Cell Biol **102**:343–352, 1986.
36. Crozat A, Penhoat A, Saez JM. Processing of angiotensin II (A-II) and (Sar^1, Ala^8) A-II by cultured bovine adrenocortical cells. Endocrinology **118**:2312–2318, 1986.
37. Bligh EG, Dyer WJ. A rapid method of total lipid extraction and purification. Can J Biochem Physiol **37**:911–917, 1959.
38. Bradford MM. A rapid and sensitive method for the quantitation

of microgram quantities of protein utilizing the principle of protein-dye binding. Anal Biochem **72**:248–254, 1976.
39. Munson PJ, Rodbard D. LIGAND: A versatile computerized approach for characterization of ligand-binding systems. Anal Biochem **107**:220–239, 1980.
40. Lemire JM, Covin CW, White S, Gianchelli CM, Schwartz SM. Characterization of cloned aortic smooth muscle cells from young rats. Am J Pathol **144**:1068–1081, 1994.
41. Natarajan R, Gu J-L, Rossi J, Gonzales N, Lanting L, Xu L, Nadler J. Elevated glucose and angiotensin II increase 12-lipoxygenase activity and expression in porcine aortic smooth muscle cells. Proc Natl Acad Sci USA **90**:4947–4951, 1993.
42. Molloy CJ, Taylor DS, Weber H. Angiotensin II stimulation of rapid protein tyrosine phosphorylation and protein kinase activation in rat aortic smooth muscle cells. J Biol Chem **268**:7338–7345, 1993.
43. Molloy CJ. Novel signal transduction targets in cardiovascular disease: Role of platelet-derived growth factor in vascular smooth muscle cell proliferation. Drug Dev Res **29**:148–157, 1993.
44. Weber H, Taylor DS, Molloy CJ. Angiotensin II induces delayed mitogenesis and cellular proliferation in rat aortic smooth muscle cells. J Clin Invest **93**:788–798, 1994.
45. Weber H, Webb ML, Serafino R, Taylor DS, Moreland S, Norman J, Molloy CJ. Endothelin-1 and angiotensin-II stimulate delayed mitogenesis in cultured rat aortic smooth muscle cells: Evidence for common signaling mechanisms. Mol Endocrinol **8**:148–158, 1994.
46. Nakano T, Higashino K, Kikuchi N, Kishino J, Nomura K, Fujita H, Ohara O, Arita H. Vascular smooth muscle cell-derived, Gla-containing growth-potentiating factor for Ca^{2+}-mobilizing growth factors. J Biol Chem **270**:5702–5705, 1995.
47. Nickenig G, Murphy TJ. Downregulation of vascular smooth muscle angiotensin receptor gene expression by growth factors. Mol Pharmacol **46**:653–659, 1994.
48. Sandberg K. Structural analysis and regulation of angiotensin II receptors. Trends Endocrinol Metab **5**:28–35, 1994.
49. Paxton WG, Marrero MB, Klein JD, Delafontaine P, Berk BC, Bernstein KE. The angiotensin II AT_1 receptor is tyrosine and serine phosphorylated and can serve as a substrate for the Src family of tyrosine kinases. Biochem Biophys Res Commun **200**:260–267, 1994.
50. Vener AV, Loeb J. Zinc-induced tyrosine phosphorylation of hippocampal $p60^{c\text{-}Src}$ is catalyzed by another protein tyrosine kinase. FEBS Lett **308**:91–93, 1992.
51. Han C, Abel PW, Minneman KP. α_1-adrenoceptor subtypes linked to different mechanisms for increasing intracellular Ca^{2+} in smooth muscle. Nature **329**:333–335, 1987.
52. Putney JW Jr. Formation and actions of calcium-mobilizing messenger, inositol 1,4,5-trisphosphate. Am J Physiol **252**: G149–G157, 1987.
53. Cotecchia S, Schwinn DA, Randall RR, Lefkowitz RJ, Caron MG, Kobilka BK. Molecular cloning and expression of the cDNA for the hamster α_1-adrenergic receptor. Proc Natl Acad Sci USA **85**:7159–7163, 1988.
54. Kemp BE, Pearson RB. Protein kinase recognition sequence motifs. Trends Biochem Sci **15**:342–346, 1990.
55. Jackson CL, Schwartz SM. Pharmacology of smooth muscle cell replication. Hypertension **20**:713–736, 1992.
56. Leduc I, Meloche S. Angiotensin II stimulates tyrosine phosphorylation of the focal adhesion-associated protein paxillin in aortic smooth muscle cells. J Biol Chem **270**:4401–4404, 1995.
57. Wilson E, Mai Q, Sudhir K, Weiss RH, Ives HE. Mechanical strain induces growth of vascular smooth muscle cells via autocrine action of PDGF. J Cell Biol **123**:741–747, 1993.